Journal of Theoretical Biology 264 (2010) 123–129

Contents lists available at ScienceDirect

Journal of Theoretical Biology

journal homepage: www.elsevier.com/locate/yjtbi

Concurrent growth of phenotypic features: A phenomenological universalities approach

L. Barberis [a,*], C.A. Condat [a,b], A.S. Gliozzi [c], P.P. Delsanto [c]

[a] FaMAF, Universidad Nacional de Córdoba, Medina Allende s/n, Ciudad Universitaria, 5000 Córdoba, Argentina
[b] IFEG, CONICET, Argentina
[c] Department of Physics, Politecnico di Torino, C. Duca degli Abruzzi 24, 10129, Torino, Italy

ARTICLE INFO

Article history:
Received 7 October 2009
Received in revised form
25 November 2009
Accepted 22 December 2009
Available online 4 January 2010

Keywords:
Growth
Ontogenesis
Allometry
Phenomenological universalities
Gompertz
Phenotypes

ABSTRACT

Different physical features of an organism are often measured concurrently, because their correlations can be used as predictors of longevity, future health, or adaptability to an ecological niche. Since, in general, we do not know a priori if the temporal variations in the measured quantities are causally related, it may be useful to have a method that could help us to identify possible correlations and to obtain parameters that may vary from population to population. In this paper we develop a procedure that may detect underlying relationships. We do this by generalizing the recently introduced concept of phenomenological universalities to the complex field. In this generalization, allometric growth is described by a complex function, whose real and imaginary parts represent two phenotypic traits of the same organism. As particular solutions of the resulting problem, we obtain generalizations of the Gompertz and the von Bertalanffy–West growth equations. We then apply the procedure to two biological systems in order to show how to determine the existence of mutual interference between trait variations.

1. Introduction

The vast experimental and modeling literature on ontogenetic growth is being continuously enriched by new extensions (Bajzer, 1999; Banavar et al., 1999; West et al., 2001; Damuth, 2001; Dodds et al., 2001; Kokshenev, 2003; Santillán, 2003; Makarieva et al., 2004; Bouvet et al., 2005; de Vladar, 2006; West and Brown, 2005; Dingli and Pacheco, 2007; Clauset and Erwin, 2008). These studies are not immune from controversy (Makarieva et al., 2009; Sousa et al., 2009; Zuo et al., 2009). Although equations such as those of Gompertz and von Bertalanffy have been used for many decades to obtain empirical fits to experimental results, it has been cogently argued that there are general biological mechanisms that are responsible for ontogenetic growth (West and Brown, 2005). These mechanisms appear to be at work in most living systems, including tumors (Guiot et al., 2003; Delsanto et al., 2004). More recently, Delsanto et al. generated a classification scheme for what they called *phenomenological universalities* (PUNs) (Castorina et al., 2006; see also Delsanto et al., 2008). In this classification, the Malthusian, Gompertzian, and von Bertalanffy–West equations emerge naturally as elements in a hierarchy of PUN classes, called UN (Delsanto et al., 2008; Pugno et al., 2008; Delsanto et al., 2009; Gliozzi et al., 2009).

Much less theoretical work has been devoted to investigate the correlations between simultaneous changes in two or more phenotypic features of a given specimen. Simultaneous measurements are performed and their correlations are often analyzed in order to predict the future of an organism or class of organisms. For instance, weight and intraocular pressure were measured to determine the possible correlation between obesity and glaucoma (Mori et al., 2000), height and circumference of *eucalyptus* trees were measured to investigate if the trees' plasticity for growth traits and form is under genetic control (Bouvet et al., 2005), head width and tail lengths were measured in salamander larvae to assess their phenotypic plasticity in response to predators (Michimae and Hangui, 2008), waist and hip circumferences were measured to be used as indexes of body fat distribution and studied to determine the effects of smoking (Shimokata et al., 1989b), height and weight were simultaneously determined to obtain the body-mass index (Canessa, 2007), etc.

In this work we extend the formalism of Castorina et al. (2006) to investigate the simultaneous temporal evolution of two possibly correlated physical features. The quantities representing these features are introduced as the real and imaginary parts of a complex function. This function evolves in time according to the UN formalism and permits a simultaneous fit to the two traits

* Corresponding author. Fax: +54 351 4334054.
E-mail addresses: lbarberi@famaf.unc.edu.ar (L. Barberis), condat@famaf.unc.edu.ar (C.A. Condat), antonio.gliozzi@polito.it (A.S. Gliozzi), pier.delsanto@polito.it (P.P. Delsanto).

0022-5193/$ - see front matter © 2009 Elsevier Ltd. All rights reserved.
doi:10.1016/j.jtbi.2009.12.024

considered. Although the approach we study here will involve first order time derivatives and two interacting functions, we remark that these functions should not be interpreted as populations, since, as we shall see, the genesis of the model implies a common underlying growth force.

The details of the extended formalism, which we dub complex phenomenological universalities (CUNs), are presented in Section 2. In Section 3 we apply the CUNs to analyze two of the sets of simultaneous measurements mentioned above, i.e., the temporal variations of body fat distribution in humans (Shimokata et al., 1989b) and the height and circumference of *eucalyptus* trees (Bouvet et al., 2005). In the first case, the UN classes do not give a suitable description, while the new CUNs lead to good fits, suggesting that there is a correlation between variations in the amount of fat in different body parts. In the second case, application of the CUNs does not significantly improve upon the fits generated by the UNs. This implies that the mutual influences between variations in the considered traits are either nonexistent or weak. This result, which could not have been obtained a priori, is confirmed by the small size of the parameters characterizing trait correlation. Finally, in Appendix A we test the robustness of our approach using simulated data sets.

2. The model

We wish to investigate the simultaneous evolution of two phenotypic features of an individual. The quantities describing these features will be represented by the real and imaginary parts of the complex function $Y(t)=y_1(t)+iy_2(t)$. We postulate that the evolution of $Y(t)$ is determined by a generalization of the UN growth equation (Castorina et al., 2006; Delsanto et al., 2008) to the complex field,

$$\frac{dY}{dt}=A[Y(t)]Y(t). \tag{1}$$

Following the UN formalism, we assume that the evolution rate $\dot{A}$ of the complex dynamic functional $A[Y(t)]$ can be expressed in terms of a power series of A itself,

$$\dot{A}=\sum_{n=1}^{\infty} f_n A^n, \tag{2}$$

where the coefficients f_n are generally complex. If an adequate fit is obtained by truncating the expansion at the N-th power of A, then we say that the underlying phenomenology belongs to the CUN universality class.

2.1. CU1—generalizing Gompertz

The class CU1 is obtained by truncating the expansion in Eq. (2) to the lowest order ($N=1$):

$$\dot{A}=f_1 A\equiv(\alpha_1+i\alpha_2)A, \tag{3}$$

where $\alpha\equiv(\alpha_1+i\alpha_2)=f_1$. Integrating Eq. (1), we get,

$$Y(t)=Y(0)\exp\left[-\frac{A_0}{\alpha}(1-\exp(\alpha t))\right] \tag{4}$$

Here $A_0=A_{01}+iA_{02}=A(0)$ and $Y(0)=y_{01}+iy_{02}$ give the initial values of the dynamic functional and of the phenotypic quantities of interest, respectively. By differentiating Eq. (4) we obtain the complex Gompertz differential equation,

$$\frac{dY(t)}{dt}=\alpha Y(t)\ln\left[\frac{Y(t)}{Y(\infty)}\right], \tag{5}$$

whose asymptotic steady state is given by $Y(\infty)=Y(0)\exp(A_0/\alpha)$.

To investigate the time dependence of the real and imaginary parts of the solution, we introduce the parameter $\kappa=\kappa_1+i\kappa_2\equiv-A_0/\alpha$, and define the time-dependent auxiliary functions,

$$\theta_1(t)=\kappa_1[1-\exp(\alpha_1 t)\cos\alpha_2 t]+\kappa_2\exp(\alpha_1 t)\sin\alpha_2 t \tag{6a}$$

$$\theta_2(t)=\kappa_2[1-\exp(\alpha_1 t)\cos\alpha_2 t]-\kappa_1\exp(\alpha_1 t)\sin\alpha_2 t \tag{6b}$$

The real and imaginary parts of Eq. (4) can now be expressed as

$$y_1(t)=\exp(\theta_1)[y_{01}\cos\theta_2-y_{02}\sin\theta_2] \tag{7a}$$

and

$$y_2(t)=\exp(\theta_1)[y_{01}\sin\theta_2+y_{02}\cos\theta_2] \tag{7b}$$

Eqs. (7) represent generalized, correlated Gompertz growth functions. The phase plane trajectory is generated by a combination of a time-dependent stretching, determined by Eq. (6a), and a rotation at a time-dependent rate, determined by Eq. (6b).

From Eqs. (6) we see that α_2 characterizes oscillations with a period $2\pi/|\alpha_2|$, while for $\alpha_1<0$, as in the usual Gompertz approach, $|\alpha_1|^{-1}$ determines the time scale over which these oscillations are attenuated. If $\alpha_1=0$, both solutions are periodic functions of the time and the trajectory in the y_1–y_2 phase plane is a closed loop.

Since the coupling between y_1 and y_2 is given by the imaginary parts of the parameters α and κ, we may call α_2 and κ_2 the coupling parameters of the system. By taking $\alpha_2=\kappa_2=0$, we readily verify that both functions become uncoupled and recover conventional Gompertzian dynamics:

$$y_i(t)=y_{0i}\exp\{\kappa_1[1-\exp(\alpha_1 t)]\}, \tag{8}$$

for $i=1,2$. If $\alpha_1<0$, the parameter κ_1 determines the asymptotic values of the functions $y_i(t)$. The trajectory in the (y_1,y_2)—phase plane is a straight segment whose slope is y_{02}/y_{01}.

The complex dimensionless parameter $\kappa=-A_0/\alpha$ is a measure of the initial value of the dynamic functional in terms of characteristic times. In particular, if $\alpha_1<0$, the asymptotic values of both components are,

$$y_1(\infty)=e^{\kappa_1}(\cos\kappa_2 y_{01}-\sin\kappa_2 y_{02}) \tag{9a}$$

$$y_2(\infty)=e^{\kappa_1}(\sin\kappa_2 y_{01}+\cos\kappa_2 y_{02}) \tag{9b}$$

The final state $(y_1(\infty),y_2(\infty))$ can thus be obtained by combining the stretching (or compression) of the initial vector (y_{01},y_{02}) by a factor of $\exp(\kappa_1)$ and a rotation by an angle κ_2. The parameter κ_2 determines the overall component admixture, which is maximal for $\kappa_2=\pi/2$ and zero for $\kappa_2=0$. Therefore, α_2 and κ_2 can be used as parameters that characterize the correlation strength.

A different perspective ensues if we look at the real and imaginary parts of the differential equation. If we define,

$$\psi_1(t)=A_{01}\cos\alpha_2 t-A_{02}\sin\alpha_2 t \tag{10a}$$

$$\psi_2(t)=A_{01}\sin\alpha_2 t+A_{02}\cos\alpha_2 t \tag{10b}$$

we easily obtain:

$$\frac{dy_1}{dt}=\exp(\alpha_1 t)[\psi_1 y_1-\psi_2 y_2] \tag{11a}$$

$$\frac{dy_2}{dt}=\exp(\alpha_1 t)[\psi_2 y_1+\psi_1 y_2] \tag{11b}$$

Evidently, this antisymmetric equation system yields a rich set of solutions, which will be analyzed in detail elsewhere. Here we just remark that, for instance, for those time stretches for which both $\psi_1>0$ and $\psi_2>0$, both traits are self-activating, while y_1 cross-activates y_2 and y_2 cross-inhibits y_1.

Eqs. (11) are linear equations with time-dependent coefficients. These coefficients couple the evolution of the two traits

already at the linear level. The CUN equations are therefore fundamentally different from those obtained from population models. In these models the coefficients are usually time independent and, with a few exceptions, such as the Eberhardt model, the interactions emerge only in the nonlinear terms (Turchin, 2003).

The robustness of our method is explored in Appendix A, where two artificial data sets, constructed for strong and weak interactions, respectively, are used to study the applicability of the procedure to systems having large experimental errors. There we show that the method is indeed very robust, and thus we can calculate the model parameters with high accuracy.

2.2. CU2—generalizing von Bertalanffy–West

Next, we truncate the expansion in Eq. (2) to the second order ($N=2$):

$$\dot{A} = f_1 A + f_2 A^2 \equiv \alpha A + \gamma A^2. \tag{12}$$

Here $\alpha=\alpha_1+i\alpha_2$ and $\gamma=\gamma_1+i\gamma_2$. Integrating, we find,

$$A(t) = \frac{\alpha A_0 e^{\alpha t}}{\alpha+\gamma A_0(1-e^{\alpha t})}. \tag{13}$$

Eq. (1) can now be integrated, yielding

$$Y(t) = Y(0)\left[1+\frac{\gamma A_0}{\alpha}(1-\exp(\alpha t))\right]^{-1/\gamma}. \tag{14}$$

Eq. (14) solves the generalized complex von Bertalanffy–West equation,

$$\frac{dY(t)}{dt} = aY^{1+\gamma}(t)\left\{1-\left[\frac{Y(t)}{Y(\infty)}\right]^{-\gamma}\right\} \tag{15}$$

Here $a=[Y(0)]^{-\gamma}[A_0+\alpha/\gamma]$ and the steady state is given by

$$Y(\infty) = Y(0)\left[1+\frac{\gamma A_0}{\alpha}\right]^{-1/\gamma} \tag{16}$$

It is convenient to rewrite Eq. (14) using polar coordinates,

$$Y(t) = Y(0)[r(t)e^{i\Theta(t)}]^{-1/\gamma}. \tag{17}$$

By defining the parameter $k=k_1+ik_2=\gamma A_0/\alpha$, we obtain the following expressions for the amplitude $r(t)$ and the phase $\Theta(t)$:

$$r = \{(1+k_1)^2+k_2^2+2e^{\alpha_1 t}[k_2\sin\alpha_2 t - k_1\cos\alpha_2 t - (k_1^2+k_2^2)\cos\alpha_2 t] + e^{2\alpha_1 t}(k_1^2+k_2^2)\}^{1/2} \tag{18}$$

$$\Theta = arctg\left[\frac{k_2 - e^{\alpha_1 t}(k_2\cos\alpha_2 t + k_1\sin\alpha_2 t)}{1+k_1+e^{\alpha_1 t}(k_2\sin\alpha_2 t - k_1\cos\alpha_2 t)}\right]. \tag{19}$$

Defining the auxiliary function

$$\xi(t) = \frac{\gamma_2\ln r - \gamma_1\Theta}{\gamma_1^2+\gamma_2^2}, \tag{20}$$

we can write the real and imaginary parts of the solution as,

$$y_1(t) = \exp\left(-\frac{\gamma_1\ln r+\gamma_2\Theta}{\gamma_1^2+\gamma_2^2}\right)(y_{01}\cos\xi - y_{02}\sin\xi) \tag{21a}$$

$$y_2(t) = \exp\left(-\frac{\gamma_1\ln r+\gamma_2\Theta}{\gamma_1^2+\gamma_2^2}\right)(y_{01}\sin\xi + y_{02}\cos\xi) \tag{22b}$$

If $\alpha_1<0$, both species reach a steady state, for which,

$$r_s = [(1+k_1)^2+k_2^2]^{1/2}; \quad \Theta_s = arctg\left(\frac{k_2}{1+k_1}\right) \tag{23}$$

If $\gamma_2=\alpha_2=A_{02}=0$, then $k_1=\gamma A_{01}/\alpha_1$ and $k_2=0$. Therefore, from Eqs. (19) and (20), $\Theta=\xi=0$ and we recover the usual U2 result (West et al., 2001; Castorina et al., 2006):

$$y_j(t) = [1+k_1(1-e^{\beta_1 t})]^{-1/\gamma_1}y_{0j}, \quad j=1,2 \tag{24}$$

In this case, both components evolve independently, following the conventional von Bertalanffy–West law.

The parameters α_1 and α_2 have the same meaning as in CU1. The coupling between y_1 and y_2 is given by the imaginary parts of the parameters α, k, and γ. In the conventional von Bertalanffy–West problem, the parameter γ is associated with the energy absorption mode. For instance, $\gamma=1/4$ corresponds to a fractal resource distribution, which has been proposed to be responsible for growth in many organisms (West et al., 2001) and $\gamma=1/3$ corresponds to a diffusive energy flux, which has been suggested to be rate-determining in the growth of multicellular tumor spheroids (Menchón and Condat, 2006). Here, we can ascribe a similar meaning to γ_1, although the interpretation of γ_2 is likely to depend on the particular problem under scrutiny. The influence of the parameters k_1 and k_2 is similar to that of κ_1 and κ_2 in CU1, although the trajectories in the phase plane are more complicated and will be discussed elsewhere.

3. Two applications

Growth-related quantities are frequently fitted using either the Gompertz or the von Bertalanffy–West functions, which arise naturally from the ordinary UN formalism. But there are some growth-related time-dependent quantities that do not obey these laws. We have found that there are instances in which these apparent deviations from universality can be explained by using a CUN approach. In these circumstances, we suggest that the presence of an underlying CUN-like behavior is a strong indication of the existence of correlations between the modifications in the corresponding traits. More precisely, the CUN formalism can be directly used to quantify the intensity of the mutual influence between traits. In this Section we discuss the results of two sets of experiments in which it is impossible to establish a priori whether such an interaction is present or relevant. In the first example we find a strong interaction between the traits, while in the second example we show that the mutual influence is either weak or nonexistent.

3.1. Distribution of body fat in humans

Since the pattern of body fat distribution is known to be related to a number of clinically relevant variables, Shimokata et al. (1989a) studied five anthropometric ratios (waist–arm ratio, waist–hip ratio, etc.) for 1179 men and women, and organized their results according to their subjects' ages. Here we analyze the data for the simultaneous measurements of waist and arm circumference in men. In Fig. 1 we present three sets of fits to averages of Shimokata's measurements of the arm circumference. A priori we can argue that the nonmonotonicity of the data would make it impossible for either a Gompertz or a von Bertalanffy–West function to provide an adequate description. This is confirmed by the unsatisfactory fits generated by U1 (solid line) and U2 (not shown). Using the CU1 functions, on the other hand, we obtain a suitable simultaneous fit to both the arm (dot-dashed line) and the waist circumferences in terms of the generalized Gompertz functions. CU2 yields an even better fit (dashed line).

The simultaneous arm and waist fits obtained by means of CU1 and CU2 are displayed in Figs. 2a and b, respectively. The importance of the correlation is indicated by the presence of sizable correlation parameters α_2 and κ_2, and, in the case of CU2, γ_2 (see caption). To allow for uncertainties in the initial values, y_{01} and y_{02} (corresponding to 20-year-old males) have been treated

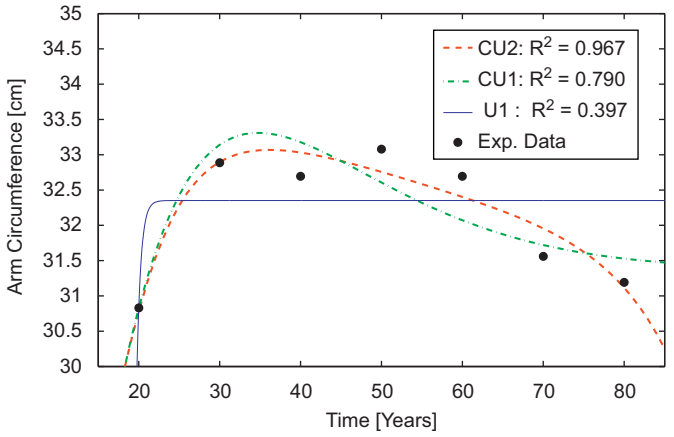

Fig. 1. Three fits to the Shimokata et al. (1989a) data (full circles) on the temporal variation of arm circumference in human males. The solid line corresponds to a regular U1 (Gompertz) curve; the dot-dashed and the dashed lines correspond, respectively, to CU1 and CU2 fits, where the companion trait (not shown) is the waist circumference. U1 fails to describe the observed behavior. The U1 parameters are $\alpha=-2.03$ (1/year) and $\kappa=0.0482$. CU1 and CU2 parameters are given in the caption to Fig. 2. The values of the coefficient of determination R^2 are specified in the figure.

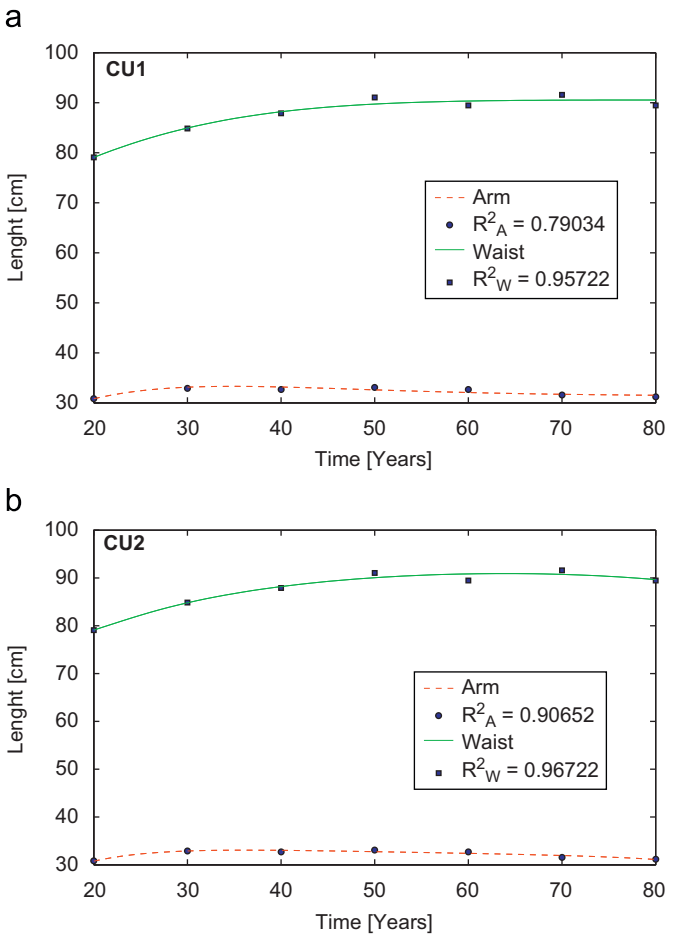

Fig. 2. (a) Simultaneous CU1 fits to the Shimokata et al. (1989a) data on the temporal variation of human male waist and arm circumferences. Parameters are: $\alpha_1=-0.0714$ (1/year), $\alpha_2=0.0358$ (1/year), $\kappa_1=0.121$, $\kappa_2=0.0378$, $y_{01}=30.8$ cm, and $y_{02}=79.1$ cm. (b) CU2 fits to the same data. Here $\alpha_1=-0.0229$ (1/year), $\alpha_2=-0.0560$ (1/year), $\kappa_1=0.247$, $\kappa_2=0.537$, $\gamma_1=-4.23$, $\gamma_2=2.75$, $y_{01}=31.0$ cm, and $y_{02}=79.1$ cm.

as adjustable parameters. However, the results of the optimization are very close to the data corresponding to $t=20$ years, confirming the consistency of the fits. The CU2 fit (Fig. 2b) is better than its CU1 counterpart, but at the expense of introducing two new parameters.

In simple biological problems, growth rates are usually taken to be constant. From Eq. (1) and $A=A_1+iA_2$ we find that we can identify two growth rate components in the CUNs. In the CU1 description, a simple computation shows that at short times ($\alpha_2 t \ll 1$) the real component $A_1(t)$ represents the "intrinsic" growth rate, i.e., the rate at which each trait would evolve if there were no correlations, while the imaginary component $A_2(t)$ indicates the evolution of the mutual influence between traits. Later on, due to the relatively large value of α_2, both components contain a substantial admixture of intrinsic and crossed contributions. At long times, both components decrease exponentially, with a time constant $|\alpha_1|^{-1}$, which would eventually lead to change cessation (in this example, beyond human life expectancy).

3.2. Allometry of tropical eucalyptus trees

As an example of noninteracting traits, we investigate the data of Bouvet et al. (2005). These authors carried out experiments with two types of tropical *eucalyptus* hybrids, measuring their height and circumference in order to assess the influence of tree density and to decide if the phenotypic plasticity for growth traits in this species is under genetic control. In Fig. 3 we show independent U1 fits for height and circumference of trees in an experiment (what we call series *t*6 in Table 1). The results obtained using CU1 and CU2 are visually indistinguishable from those for U1 and we do not show them (the R^2 values corresponding to U1, CU1 and CU2 are almost the same). The parameters obtained with U1 and CU1 are given in the upper row of Table 1. The CU1 coupling constants, α_2 and κ_2, are in all cases very small in comparison with the corresponding real parts, suggesting that circumference and height modifications are very weakly related, if at all. By looking at the table, we also find that α_1 (CU1) has the same value as α_H (U1), while the value of κ_1 (CU1) is very close to that of κ_H (U1), corresponding to height (we remind the reader that in the limit α_2, $\kappa_2 \to 0$ the CU1 formalism yields a U1 Gompertzian with parameters α_1 and κ_1).

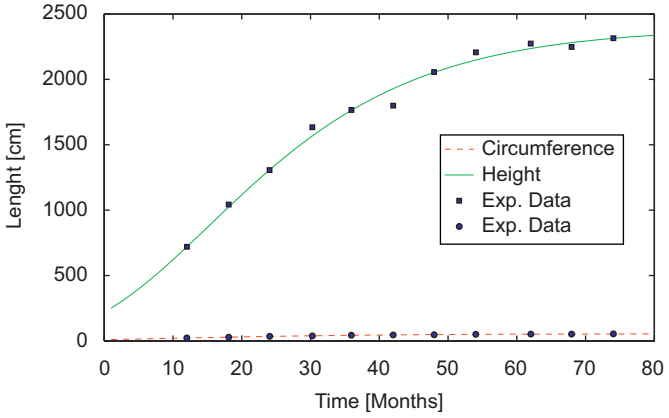

Fig. 3. Two independent U1 (Gompertzian) fits to the Bouvet et al. (2005) data on *eucalyptus* growth. The data correspond to series t6 in table 1. Both the fits to the tree height and to its circumference are very good, with coefficients of determination $R_C^2=0.997$ and $R_H^2=0.991$ for the circumference and height, respectively. The superimposed small oscillations are probably due to environmental fluctuations and, as such, cannot be described by either the UN or the CUN procedures. CU1 and CU2 fits do not exhibit any significant improvements. The initial values are $y_{0C}=22.25$ cm and $y_{0H}=720$ cm. For the other parameter values see Table 1.

Table 1
Parameters obtained by fitting four species of *eucalyptus* (coded by *t*,*r*,*x* and *c*) growing under different environmental conditions (coded by 6, 11 and 25) using U1 and CU1.

Series code	CU1				U1			
	α_1	α_2	κ_1	κ_2	Height		Circumference	
					α_H	κ_H	α_C	κ_C
t6	−0.0571	−0.000096	1.2202	0.0079	−0.0571	1.2024	−0.0543	0.9043
t11	−0.0400	0.000145	1.2547	0.0063	−0.0400	1.2549	−0.0492	0.9922
t25	−0.0359	−0.000083	1.1333	0.0070	−0.0359	1.1334	−0.0374	0.8163
r6	−0.0512	−0.000142	1.3092	0.0079	−0.0512	1.3094	−0.0503	1.0574
r11	−0.0403	0.000205	1.1984	0.0038	−0.0030	1.1985	−0.0446	0.9318
r25	−0.0424	−0.000095	0.8743	0.0035	−0.0434	0.0874	−0.0368	0.7037
x6	−0.0530	−0.000104	1.2589	0.0038	−0.0530	1.2590	−0.0423	1.1203
x11	−0.0348	−0.000009	1.2155	0.0036	−0.0395	1.2156	−0.0351	1.0618
x25	−0.0338	−0.000056	0.9342	0.0029	−0.0394	0.9343	−0.0364	0.7865
c6	−0.0557	0.000011	1.2256	0.0075	−0.0559	1.2258	−0.0602	0.9149
c11	−0.0492	0.000033	0.0940	0.0058	−0.0492	0.9400	−0.0557	0.6709
c25	−0.3860	−0.000050	0.7894	0.0047	−0.0386	0.7896	−0.0377	0.5475

Note the similitude between α_1 (CU1) and α_C and α_H (U1). The parameter κ_1 is very close to κ_H (which characterizes height variations); due to the influence of the small but nonvanishing κ_2 (CU1) we obtain a lower value of κ_C than that predicted in the limit $(\alpha_2,\kappa_2)\to 0$.

We do not have data for the values of y_1 and y_2 at the planting time, but a U1 extrapolation gives very reasonable results: height = 2.4 m and circumference = 0.11 m.

Table 1, which exhibits the data corresponding to four species of *eucalyptus* growing under different conditions, confirms the robustness of our results. In all cases the U1 parameters α_H and α_C, characterizing height and circumference growth, respectively, are numerically very close to each other, suggesting the existence of an underlying growth mechanism that affects similarly height and circumference. We also remark that these values (especially α_H) are very close to the CU1 parameter α_1. The same considerations apply to the intrinsic parameters κ_H and κ_C (U1), and κ_1 (CU1). The correlation parameters α_2 and κ_2 are always very small, confirming that both traits evolve independently from each other. The initial values y_{0H} and y_{0C} (corresponding to 12 month-old trees) obtained from the fit coincide to three significant figures with the experimental data.

Since $\alpha_2 t \ll 1$ over the whole length of the experiment, $A_1(t)$ and $A_2(t)$ represent, respectively, the direct growth and the (weak) mutual influence between traits over the whole time range. Specifically, the smallness of A_2 means that length growth is not correlated to circumference growth.

Despite having more available parameters, fits carried out using U2 or CU2 yield similar values of the coefficient R^2 to those obtained from their U1 and CU1 counterparts, which indicates that *eucalyptus* growth is indeed Gompertzian.

4. Discussion

The temporal changes in two traits of the same individual may be either completely independent or correlated. The CUNs introduced in this paper are adequate tools to investigate correlated growth processes, which cannot be described by the ordinary (UN) growth laws. We have illustrated the formalism with two applications. In the case of the *eucalyptus* trees we have shown that the dynamics of two growth indicators (circumference and height) can be described by usual Gompertz functions, their correlations being very weak. This means that there is a separate underlying growth mechanism responsible for the variations in both traits. The examples analyzed here correspond to trees that exhibit phenotypic plasticity. We are currently studying the possible dependence of phenotypic plasticity on the strength of the correlation between trait variations. In the case of human body fat, on the other hand, separate growth equations are inadequate and we must resort to the CUNs to obtain a satisfactory description, which suggests that the corresponding trait variations are strongly correlated.

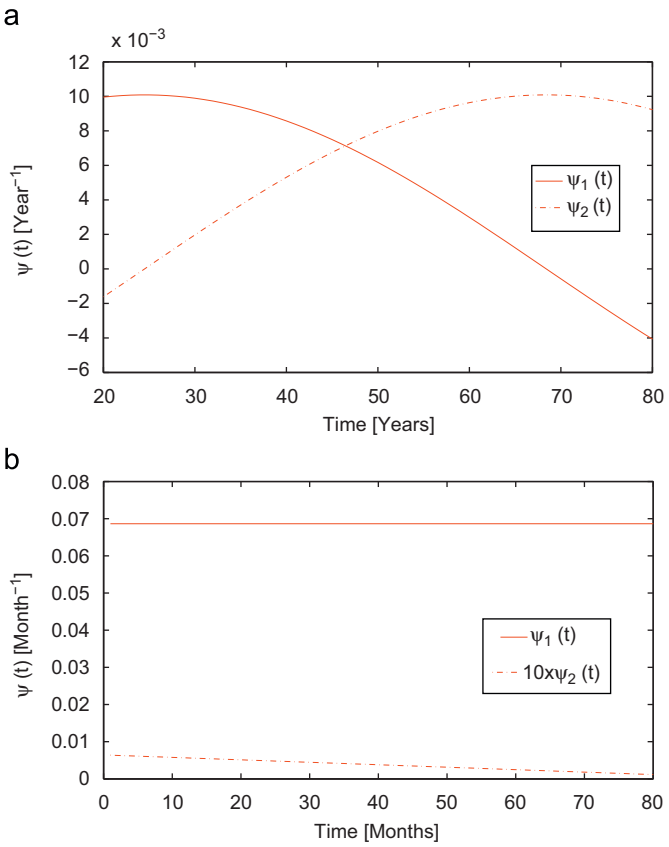

Fig. 4. Time dependence of the activation functions ψ_1 and ψ_2 for (a) fat distribution in human males and (b) *eucalyptus* perimeter and height. The relatively large values of ψ_2 in Fig. 4a are responsible for a strong trait interaction in the first case, which is absent in the latter.

The examples discussed in this paper are further clarified by an application of Eqs. (11). The functions ψ_1 and ψ_2, which we plot in

Fig. 4, determine the influence that each trait has on the other. For human body fat (panel a), both traits have intrinsic activation ($\psi_1 > 0$), except for the latest stages (> 68 years), while, since $\psi_2 > 0$ (except at the very beginning), y_2 (waist) has a negative influence on y_1 (arm). This influence is responsible for the observed decrease in arm circumference after the age of 50 years. The arm perimeter, y_1, on the other hand, has a positive influence on y_2. At long times, the decaying exponential prefactor in Eqs. (11) is responsible for the disappearance of changes in the observed traits. The situation depicted in panel (b), which corresponds to *eucalyptus* growth, is quite different. The almost constant, positive ψ_1 means that variations in both circumference and height are controlled by the exponential prefactor. The small size of ψ_2 is responsible for the very weak correlation between the measured *eucalyptus* traits.

Acknowledgments

This work was supported by SECyT-UNC (Project no. 05/B354), ANPCyT (PICT 2205/33675), and CONICET (PIP 6311/05) (Argentina). AG wishes to acknowledge the Regione Piemonte for the post-doc fellowship support.

Appendix A. Robustness of the numerical approach

In many biological and biomedical applications the experimental errors may be rather large. The question then arises of the applicability of the approach in such a case. To answer this question we propose the following numerical experiment: we consider two datasets, generated by means of Eq. (7) for the Gompertzian evolution of two correlated quantities y_1 and y_2 (called in the following the "*exact*" values). Conforming to the two applications discussed in the paper, the two datasets will refer, respectively, to large and small interferences between the main variables.

We then assume a variable amplitude B for the error bar and call "*experimental*" data the values of $y_1(t)$ and $y_2(t)$ obtained by adding, at each time t, an amount rB to the "exact" values, where r represents a random Gaussian-distributed number with mean value 0 and standard deviation 1. Finally, we call "*theoretical*" results the values of $y_1(t)$ and $y_2(t)$ obtained by applying the CU1 procedure to the "experimental" data.

A frequently adopted criterion to evaluate the quality of a fitting procedure is the so-called R^2, defined, in the case of a single variable y, as

$$R^2 = 1 - \frac{\sum_{p=1}^{P}(y_p - \tilde{y}_p)^2}{\sum_{p=1}^{P}(y_p - \overline{y}_p)^2}, \tag{A.1}$$

where $\overline{y} = P^{-1}\sum_{p=1}^{P} y_p$, P is the number of experimental points included in the dataset, y_p are the "experimental" values of the variable y, and $\tilde{y}_p$ the corresponding values obtained by the fitting procedure.

Ideally, R^2 should be equal to one. Its value, however, decreases, for two reasons:

- $\tilde{y}(t)$ is not the best fitting function;
- the experimental error bars introduce in the numerator in Eq. (A.1) terms such as $(y_p - \tilde{y}_p) \neq 0$, which lower R^2 down to a value R_E^2.

Obviously, the procedure must be, in the present situation, generalized to the case of two interacting variables.

In Figs. 5a and b we plot the behavior of R^2 vs. B for the two cases considered (large and small interference between y_1 and y_2). It can be easily seen that even for not too large values of B, R^2 decreases quite fast: e.g. for B=10% of the corresponding y_i, $R^2 \approx 0.75$ for y_1 and < 0.6 for y_2. These low values of R^2 can be, however, attributed completely to the building up of

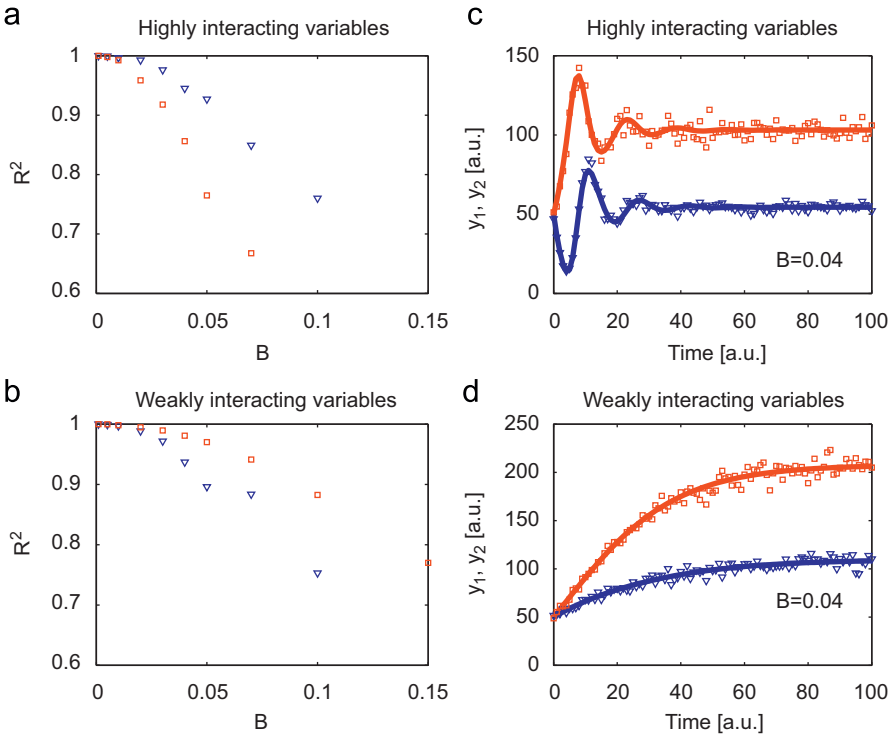

Fig. 5. (a) and (b) plots of R^2, as defined in Eq. (A1), vs. the amplitude B (in % of the corresponding y_i) of the error bars for two different choices of the interaction a_{12}, i.e. (a) k_1=0.5, k_2=0.3, $\alpha_1 = -0.1$, $\alpha_2 = -0.4$; (b) k_1=1.2, k_2=0.3, $\alpha_1 = -0.05$, $\alpha_2 = -0.005$. In all cases triangles refer to y_1 and squares to y_2. Figs. 5(c) and (d) report the corresponding CU1 curves, $\tilde{y}_1(t)$ and $\tilde{y}_2(t)$, which are virtually indistinguishable from the corresponding "exact" curves $y_1(t)$ and $y_2(t)$.

experimental errors in R_E^2 (second reason above). In fact, if we plot the values $\tilde{y}_1$ and $\tilde{y}_2$ vs. time obtained by means of the CU1 procedure (see Figs. 5c and d), the resulting values are almost completely identical with the corresponding exact values. Indeed, in the plot they cannot be distinguished. To conclude, from a numerical point of view, the procedure presented in this paper is remarkably robust, even for rather large values of the error bars.

References

Bajzer, Z., 1999. Gompertzian growth as a self-similar and allometric process. Growth, Development & Aging 63, 3–11.

Banavar, J.R., Maritan, A., Rinaldo, A., 1999. Size and form in efficient transportation networks. Nature 399, 130–132.

Bouvet, J.M., Vigneron, P., Saya, A., 2005. Phenotypic plasticity of growth trajectory and ontogenic allometry in response to density for Eucalyptus hybrid clones and families. Ann. Bot. 96, 811–821.

Canessa, E., 2007. Modeling of body mass index by Newton's second law. J. Theor. Biol. 248, 646–656, doi:10.1016/j.jtbi.2007.06.011.

Castorina, P., Delsanto, P.P., Guiot, C., 2006. A classification scheme for phenomenological universalities in growth problems. Phys. Rev. Lett. 96, 188701 1–4.

Clauset, A., Erwin, D.H., 2008. The evolution and distribution of species body size. Science 321, 399–401.

Damuth, J., 2001. Scaling of growth: plants and animals are not so different. Proc. Natl. Acad. Sci. 98, 2113–2114.

Delsanto, P.P., Guiot, C., Degiorgis, P.G., Condat, C.A., Mansury, Y., Deisboeck, T.S., 2004. A growth model for multicellular tumor spheroids. Appl. Phys. Lett. 85, 4225–4227.

Delsanto, P.P., Gliozzi, A.S., Guiot, C., 2008. Scaling, growth and cyclicity in biology a new computational approach. Theor. Biol. Med. Modell. 5, 5, doi:10.1186/1742-4682-5-5.

Delsanto, P.P., Gliozzi, A.S., Bruno, C.L.E., Pugno, N., Carpinteri, A., 2009. Scaling laws and fractality in the framework of a phenomenological approach. Chaos, Solitons and Fractals 41, 2782–2786.

De Vladar, H.P., 2006. Density-dependence as a size-independent regulatory mechanism. J. Theor. Biol. 238, 245–256, doi:10.1016/j.jtbi.2005.05.014.

Dingli, D., Pacheco, J.M., 2007. Ontogenetic growth of the haemopoietic stem cell pool in humans. Proc. R. Soc. B 274, 2497–2501, doi:10.1098/rspb.2007.0780.

Dodds, P.S., Rothman, D.H., Weitz, J.S., 2001. Re-examination of the "3/4-law" of metabolism. J. Theor. Biol. 209, 9–27, doi:10.1006/jtbi.2000.2238.

Gliozzi, A.S., Guiot, C., Delsanto, P.P., 2009. A new computational tool for the phenomenological analysis of multipassage tumor growth curves. PLoS ONE 4, e5358, doi:10.1371/journal.pone.0005358.

Guiot, C., Degiorgis, P.G., Delsanto, P.P., Gabriele, P., Deisboeck, T.S., 2003. Does tumor growth follow a "universal law"? J. Theor. Biol. 225, 147–151, doi:10.1016/S0022-5193(03)00221-2.

Kokshenev, V.B., 2003. Observation of mammalian similarity through allometric scaling laws. Physica A 322, 491–505.

Makarieva, A.M., V.G. Gorshkov, V.G., Li, B.-L., 2004. Ontogenetic growth: models and theory. Ecol. Modelling 176, 15–26.

Makarieva, A.M., Gorshkov, V.G., Li, B.L., 2009. Comment on "Energy uptake and allocation during ontogeny". Science 325, 1206a.

Menchón, S.A., Condat, C.A., 2006. Ontogenetic growth of multicellular tumor spheroids. Physica A 371, 76–79.

Michimae, H., Hangui, J.-I., 2008. A trade-off between prey- and predator- induced polyphenisms in larvae of the salamander *Hynobius retardatus*. Behav. Ecol. Sociobiol. 62, 699–704, doi:10.1007/s00265-007-0494-z.

Mori, K., Ando, F., Nomura, H., Sato, Y., Shimokata, H., 2000. Relationship between intraocular pressure and obesity in Japan. Int. J. Epidemiol. 29, 661–666.

Pugno, N., F. Bosia, F., Gliozzi, A.S., Delsanto, P.P., Carpinteri, A., 2008. Phenomenological approach to mechanical damage growth analysis. Phys. Rev. E 78, 046103 1–5.

Santillán, M., 2003. Allometric scaling laws in a simple oxygen exchanging network: possible implications on the biological allometric scaling laws. J. Theor. Biol. 223, 249–257, doi:10.1016/S0022-5193(03)00097-3.

Shimokata, H., Tobin, J.D., Muller, D.C., Elahi, D., Coon, P.J., Andres, R., 1989a. Studies in the distribution of body fat: I. Effects of age, sex, and obesity. J. Gerontol. 44, M66-73.

Shimokata, H., Muller, D.C., Andres, R., 1989b. Studies in the distribution of body fat: III. Effects of cigarette smoking. JAMA 261, 1169–1173.

Sousa, T., Marques, G.M., Domingos, T., 2009. Comment on "Energy uptake and allocation during ontogeny". Science 325, 1206b.

Turchin, P., 2003. Complex Population Dynamics. Princeton University Press, Princeton (Chapter 4).

West, G.B., Brown, J.H., Enquist, B.J., 2001. A general model for ontogenetic growth. Nature 413, 628–631.

West, G.B., Brown, J.H., 2005. The origin of allometric scaling laws in biology from genomes to ecosystems: towards a quantitative unifying theory of biological structure and organization. J. Exp. Biol. 208, 1575–1592.

Zuo, W., Moses, M.E., Hou, Ch., Woodruff, W., West, G.B., Brown, J.H., 2009. Response to comments on "Energy uptake and allocation during ontogeny". Science 325, 1206c.